P. Masarati, M. Morandini, A. Fumagalli
Control Constraint of Underactuated Aerospace Systems
Journal of Computational and Nonlinear Dynamics, Vol. 9, N. 2, 2014, 021014 (9 pages)
doi:10.1115/1.4025629

Control Constraint of Underactuated Aerospace Systems

Pierangelo Masarati[*], **Marco Morandini**
Politecnico di Milano, Dipartimento di Scienze e Tecnologie Aerospaziali
Email: {pierangelo.masarati,marco.morandini}@polimi.it

Alessandro Fumagalli
Politecnico di Milano, Dipartimento di Scienze e Tecnologie Aerospaziali
now at Selex ES, a Finmeccanica Company
Space Robotics PEM/System Engineering
Email: alessandro.fumagalli@selexgalileo.com

This paper discusses the problem of control constraint realization applied to the design of maneuvers of complex underactuated systems modeled as multibody problems. Applications of interest in the area of aerospace engineering are presented and discussed. The tangent realization of the control constraint is discussed from a theoretical point of view and is used to determine feedforward control of realistic under-actuated systems. The effectiveness of the computed feedforward input is subsequently verified by applying it to more detailed models of the problems, in the presence of disturbances and uncertainties in combination with feedback control. The problems are solved using a free general-purpose multibody software that writes the constrained dynamics of multi-field problems formulated as Differential-Algebraic Equations. The equations are integrated using unconditionally stable algorithms with tunable dissipation. The essential extension to the multibody code consisted in the addition of the capability to write arbitrary constraint equations and apply the corresponding reaction multipliers to arbitrary equations of motion. The modeling capabilities of the formulation could be exploited without any undue restriction on the modeling requirements.

Introduction

A key theme in analytical mechanics is the study of constrained systems of rigid bodies, whose relative motions are mutually constrained according to a set of constraints equations. These equations represent the actual physical pairs of the system; when constraints are ideal the constraint reactions do not contribute to the virtual work.

Two main approaches are used to describe the dynamics of a constrained mechanical system. The first uses a reduced number of kinematic variables, often called "minimal coordinates", that correspond to the actual degrees of freedom of the system. The constraints equations are used 'a priori' to formulate the reduced set of coordinates, and constraint reactions do not appear explicitly. The second approach consists in writing the dynamics of each rigid body as if it were unconstrained, while explicitly adding kinematic constraint relationships in the form of algebraic equations. The constraints contribute to the equilibrium of each constrained body by means of algebraic variables that are related to the reaction forces and moments. The latter approach is considered more suitable for the study presented in this work because it eases the writing of the constraint control equations and their application to rather general and heterogeneous problems, at the cost of increased problem size.

The so called 'passive' constraint problem has been the subject of extensive work (see [1, 2] for a complete review). This term, to the authors' knowledge, was first used in [3–5]; the term 'contact' constraint is used as well [6]. The interest is on the motion of the system; the constraint reactions are treated as passive forces generated by particular elements of the system itself. It is assumed that the physical structure of the system is able to instantaneously generate the required constraints force, whatever their required value.

Some recent works dealt with the problem of actively generating the forces required to perform a particular task, e.g. tracking a desired trajectory. The resulting artificial constraints have been termed *servo-*, *active*, *control*, or *program constraints* [3–13]. The problem is quite different from the classical constrained motion problem, commonly associated to the passive constraint problem. A system equipped with a number of actuators or servos is requested to move according to a set of control constraints. The structure of the servos and of the constraint are not related to each other a priori. Only the forces and torques generated by the servos make the realization of the controlled motion possible. This problem is among the few open questions in analytical mechanics.

[*]Corresponding author: Address: Politecnico di Milano, Dipartimento di Scienze e Tecnologie Aerospaziali, via La Masa 34, 20156 Milano, Italy

ASME J. Comput. Nonlinear Dyn. January 2011 6(1), doi:10.1115/1.4025629

Problem Description

The essential formulation of the proposed approach was first presented in [14]. It is revisited here to address some of the remaining open issues, such as equivalence of redundant and minimal coordinates realizations, orthogonal realization conditions and application to non-minimum phase systems.

Consider a generic control constraint problem formulated as a constrained mechanics problem using Lagrange equations of the first kind,

$$\mathbf{M}(\mathbf{x})\ddot{\mathbf{x}} + \boldsymbol{\phi}_{/\mathbf{x}}^T \boldsymbol{\lambda} = \mathbf{f}(\mathbf{x}, \dot{\mathbf{x}}) + \mathbf{B}^T(\mathbf{x})\mathbf{u} \tag{1a}$$

$$\boldsymbol{\phi}(\mathbf{x}) = \mathbf{0} \tag{1b}$$

$$\boldsymbol{\psi}(\mathbf{x}) = \boldsymbol{\alpha}(t) \tag{1c}$$

where vector $\boldsymbol{\phi}$ contains a set of scleronomous constraint equations that represent the passive constraints of the problem ($\boldsymbol{\phi}_{/\mathbf{x}}$ indicates the partial derivative of $\boldsymbol{\phi}$ with respect to $\mathbf{x}$; in this specific case, $\boldsymbol{\phi}_{/\mathbf{x}}$ is the Jacobian matrix of equations $\boldsymbol{\phi}$); the case of rheonomous constraints is not addressed for simplicity. Vector $\boldsymbol{\psi}$ contains a set of rheonomous constraint equations, with time dependence confined in vector $\boldsymbol{\alpha}$ for simplicity. These constraints are enforced using non-collocated actuators that apply the control forces collected in vector $\mathbf{f}_\mathbf{u} = \mathbf{B}^T(\mathbf{x})\mathbf{u}$ as functions of the control inputs collected in vector $\mathbf{u}$. In control constraint realization, the number of control inputs must be equal to the number of control constraints; redundant control inputs are not considered.

Minimal Coordinate Set Realization

Consider now a transformation $\mathbf{x} = \boldsymbol{\vartheta}(\mathbf{q})$ that expresses the redundant coordinates $\mathbf{x}$ as functions of the minimal set of Lagrangian coordinates $\mathbf{q}$ of the problem, under the condition $\boldsymbol{\phi}_{/\mathbf{x}}\boldsymbol{\vartheta}_{/\mathbf{q}} \equiv \mathbf{0}$, implied by $\delta\boldsymbol{\phi} = \boldsymbol{\phi}_{/\mathbf{x}}\delta\mathbf{x} = \boldsymbol{\phi}_{/\mathbf{x}}\boldsymbol{\vartheta}_{/\mathbf{q}}\delta\mathbf{q} = \mathbf{0}$ for any arbitrary perturbation $\delta\mathbf{q}$. This transformation may not be known in closed form, although the Jacobian matrix $\boldsymbol{\vartheta}_{/\mathbf{q}}$ can be computed numerically from $\boldsymbol{\phi}_{/\mathbf{x}}$ for a given configuration $\mathbf{x}$. Methods like the Singular Value Decomposition (SVD) [15, 16] and the QR decomposition [17], for example, compute an optimal (in a least-squares sense) projection matrix $\boldsymbol{\vartheta}_{/\mathbf{q}}$ for a generic set of coordinates $\mathbf{q}$ with some degree of arbitrariness, while coordinate partitioning (e.g. [18, 19]), although non necessarily optimal, preserves the physical meaning of the minimal set coordinates $\mathbf{q}$.

A minimal set form of the problem of Eq. (1) can be formally obtained by projection,

$$\underbrace{\boldsymbol{\vartheta}_{/\mathbf{q}}^T \mathbf{M} \boldsymbol{\vartheta}_{/\mathbf{q}}}_{\hat{\mathbf{M}}} \ddot{\mathbf{q}} = \underbrace{\boldsymbol{\vartheta}_{/\mathbf{q}}^T \left(\mathbf{f} - \mathbf{M} \left(\boldsymbol{\vartheta}_{/\mathbf{q}} \dot{\mathbf{q}} \right)_{/\mathbf{q}} \dot{\mathbf{q}} \right)}_{\hat{\mathbf{f}}} + \underbrace{\boldsymbol{\vartheta}_{/\mathbf{q}}^T \mathbf{B}^T}_{\hat{\mathbf{B}}^T} \mathbf{u} \tag{2a}$$

$$\boldsymbol{\psi}(\mathbf{q}) = \boldsymbol{\alpha}(t) \tag{2b}$$

where $\ddot{\mathbf{x}} = \boldsymbol{\vartheta}_{/\mathbf{q}}\ddot{\mathbf{q}} + (\boldsymbol{\vartheta}_{/\mathbf{q}}\dot{\mathbf{q}})_{/\mathbf{q}}\dot{\mathbf{q}}$ has been used. The problem of Eqs. (2) is described by a set of Differential-Algebraic Equations (DAE) of index[1] at least 3.

[1] For a definition of the differential index of DAEs see for example [20].

The control realizability condition can be obtained by considering the second derivative of the trajectory specification equation,

$$\frac{\mathrm{d}^2\boldsymbol{\psi}}{dt^2} = \boldsymbol{\psi}_{/\mathbf{q}}\ddot{\mathbf{q}} + \left(\boldsymbol{\psi}_{/\mathbf{q}}\dot{\mathbf{q}}\right)_{/\mathbf{q}}\dot{\mathbf{q}} = \ddot{\boldsymbol{\alpha}} \tag{3}$$

and, after replacing $\ddot{\mathbf{q}}$ from Eq. (2a), by computing the corresponding control inputs $\mathbf{u}$,

$$\mathbf{u} = \left(\boldsymbol{\psi}_{/\mathbf{q}}\hat{\mathbf{M}}^{-1}\hat{\mathbf{B}}^T\right)^{-1}\left(\ddot{\boldsymbol{\alpha}} - \left(\boldsymbol{\psi}_{/\mathbf{q}}\dot{\mathbf{q}}\right)_{/\mathbf{q}}\dot{\mathbf{q}} - \boldsymbol{\psi}_{/\mathbf{q}}\hat{\mathbf{M}}^{-1}\hat{\mathbf{f}}\right). \tag{4}$$

Eq. (4) requires the local non-singularity of matrix

$$\hat{\mathbf{P}} = \boldsymbol{\psi}_{/\mathbf{q}}\hat{\mathbf{M}}^{-1}\hat{\mathbf{B}}^T, \tag{5}$$

which in general is not guaranteed (e.g. [5, 6, 8, 12]).

Redundant Coordinate Set Realization

When the problem is directly formulated according to the redundant coordinate set approach, the control realization requires to locally solve the problem

$$\begin{bmatrix} \mathbf{M} & \boldsymbol{\phi}_{/\mathbf{x}}^T & -\mathbf{B}^T \\ \boldsymbol{\phi}_{/\mathbf{x}} & \mathbf{0} & \mathbf{0} \\ \boldsymbol{\psi}_{/\mathbf{x}} & \mathbf{0} & \mathbf{0} \end{bmatrix} \begin{Bmatrix} \ddot{\mathbf{x}} \\ \boldsymbol{\lambda} \\ \mathbf{u} \end{Bmatrix} = \begin{Bmatrix} \mathbf{f} \\ -\left(\boldsymbol{\phi}_{/\mathbf{x}}\dot{\mathbf{x}}\right)_{/\mathbf{x}}\dot{\mathbf{x}} \\ \ddot{\boldsymbol{\alpha}} - \left(\boldsymbol{\psi}_{/\mathbf{x}}\dot{\mathbf{x}}\right)_{/\mathbf{x}}\dot{\mathbf{x}} \end{Bmatrix} \tag{6}$$

which yields (see for example [18])

$$\mathbf{u} = \mathbf{P}^{-1}\left(\ddot{\boldsymbol{\alpha}} - \left(\boldsymbol{\psi}_{/\mathbf{x}}\dot{\mathbf{x}}\right)_{/\mathbf{x}}\dot{\mathbf{x}} - \mathbf{Q}_\mathbf{x}\left(\boldsymbol{\phi}_{/\mathbf{x}}\dot{\mathbf{x}}\right)_{/\mathbf{x}}\dot{\mathbf{x}} - \mathbf{Q}_\mathbf{f}\mathbf{f}\right) \tag{7}$$

with

$$\mathbf{P} = \boldsymbol{\psi}_{/\mathbf{x}}\left(\mathbf{I} - \mathbf{M}^{-1}\boldsymbol{\phi}_{/\mathbf{x}}^T\left(\boldsymbol{\phi}_{/\mathbf{x}}\mathbf{M}^{-1}\boldsymbol{\phi}_{/\mathbf{x}}^T\right)^{-1}\boldsymbol{\phi}_{/\mathbf{x}}\right)\mathbf{M}^{-1}\mathbf{B}^T \tag{8a}$$

$$\mathbf{Q}_\mathbf{x} = \psi_{/\mathbf{x}}\mathbf{M}^{-1}\boldsymbol{\phi}_{/\mathbf{x}}^T\left(\boldsymbol{\phi}_{/\mathbf{x}}\mathbf{M}^{-1}\boldsymbol{\phi}_{/\mathbf{x}}^T\right)^{-1} \tag{8b}$$

$$\mathbf{Q}_\mathbf{f} = \boldsymbol{\psi}_{/\mathbf{x}}\left(\mathbf{I} - \mathbf{M}^{-1}\boldsymbol{\phi}_{/\mathbf{x}}^T\left(\boldsymbol{\phi}_{/\mathbf{x}}\mathbf{M}^{-1}\boldsymbol{\phi}_{/\mathbf{x}}^T\right)^{-1}\boldsymbol{\phi}_{/\mathbf{x}}\right)\mathbf{M}^{-1} \tag{8c}$$

Matrix $\mathbf{P}$ must be invertible, much like matrix $\hat{\mathbf{P}}$. The proof of the equivalence of the two control realizability forms is given in Appendix.

Considerations on Control Realization

As discussed in [14] and citations therein, matrix $\mathbf{B}$ (and thus $\hat{\mathbf{B}}$) can be decomposed in a portion $\mathbf{B}_\perp$ (resp. $\hat{\mathbf{B}}_\perp$), which, through the inverse of the mass matrix after enforcing compliance with the passive constraints, is parallel to the subspace of $\mathbf{x}$ orthogonal to the manifold of the constraints, $\boldsymbol{\psi}_{/\mathbf{x}}$ (resp. $\boldsymbol{\psi}_{/\mathbf{q}}$), and a portion $\mathbf{B}_\parallel$ (resp. $\hat{\mathbf{B}}_\parallel$), which is tangent to the same manifold (matrix $\mathbf{P}$ of Eq. (8a), or $\hat{\mathbf{P}}$ of Eq. (5)). The decomposition of matrix $\mathbf{B} = \mathbf{B}_\perp + \mathbf{B}_\parallel$ can be obtained, for example, by considering a QR decomposition of $\boldsymbol{\psi}_{/\mathbf{x}}^T$, namely

$$\boldsymbol{\psi}_{/\mathbf{x}}^T = \mathbf{Q}\mathbf{R} = \begin{bmatrix} \mathbf{Q}_1 & \mathbf{Q}_2 \end{bmatrix}\begin{bmatrix} \mathbf{R}_1 \\ \mathbf{0} \end{bmatrix} = \mathbf{Q}_1\mathbf{R}_1, \tag{9}$$

ASME J. Comput. Nonlinear Dyn. January 2011 6(1), doi:10.1115/1.4025629

where $\mathbf{Q}$ is a unitary matrix and $\mathbf{R}_1$ is an upper triangular matrix; $\mathbf{Q}_2$ are directions in the space of the coordinates that do not affect the control constraints, i.e. $\boldsymbol{\psi}_{/\mathbf{x}}\mathbf{Q}_2 \equiv \mathbf{0}$. Then $\mathbf{B}_\perp^T = \mathbf{Q}_1\mathbf{W}_1$ and $\mathbf{B}_\parallel = \mathbf{Q}_2\mathbf{W}_2$, with $\mathbf{W}_1 = \mathbf{Q}_1^T\mathbf{B}^T$ and $\mathbf{W}_2 = \mathbf{Q}_2^T\mathbf{B}^T$. When $\mathbf{B}_\perp$ is full row rank (alternatively: when the square matrix $\mathbf{W}_1$ is full rank, as the number of rows of $\mathbf{W}_1$ is equal to the number of columns of $\mathbf{Q}_1$, which in turn is equal to the number of control constraints $\boldsymbol{\psi}$, and thus equal to the number of control inputs), the constraint can be directly enforced by the control forces $\mathbf{u}$ of Eq. (6) or (4). When $\mathbf{B}_\perp \neq \mathbf{0}$ and $\mathbf{B}_\parallel \neq \mathbf{0}$, matrix $\mathbf{B}$ projects the input vector $\mathbf{u}$ along both the orthogonal and tangent directions with respect to the constraint manifold, resulting in a non-ideal orthogonal realization [6]. As long as matrix $\mathbf{B}_\perp$ is full row rank, the constraint can be regulated by adjusting the value of $\mathbf{u}$ to ensure that the orthogonal component assumes the required value. This is sometimes called non-ideal orthogonality, since the control force also influences the unconstrained directions. When $\mathbf{B}_\perp$ is not full row rank, the input vector $\mathbf{u}$ can directly regulate only a subset of the constraint condition. In the limit case of $\mathbf{B}_\perp \equiv \mathbf{0}$, the input vector $\mathbf{u}$ is projected only along directions locally parallel to the constraint manifold. As a consequence, when $\mathbf{B}_\perp$ is not full row rank the constraint cannot be directly enforced. In this case, the differential index i of the DAE problem is higher than 3. It is also worth noting that the motion $\boldsymbol{\alpha}(t)$ prescribed using the control constraint must be at least C^{i-1} with respect to the time t (see for example [13]). The proposed condition on the rank of matrix $\mathbf{B}_\perp$ is alternative to the one on matrix $\mathbf{P}$ presented by Blajer [6], with the advantage of only requiring the comparison of the subspaces of $\mathbf{x}$ spanned by matrix $\boldsymbol{\psi}_{/\mathbf{x}}$ and $\mathbf{B}$. The following section illustrates how the problem of tangent control realization can be numerically solved using implicit numerical integration.

Numerical Aspects of Generic DAE Problem Solution

The problem of Eqs. (1) can be generically cast in the form of an implicit set of equations $\mathbf{g}(\mathbf{y},\dot{\mathbf{y}},\ddot{\mathbf{y}},t) = \mathbf{0}$, with $\mathbf{y} = \{\mathbf{x};\boldsymbol{\lambda};\mathbf{u}\}$. A local linearization

$$\delta\mathbf{g} = \mathbf{g}_{/\mathbf{y}}\delta\mathbf{y} + \mathbf{g}_{/\dot{\mathbf{y}}}\delta\dot{\mathbf{y}} + \mathbf{g}_{/\ddot{\mathbf{y}}}\delta\ddot{\mathbf{y}} \tag{10}$$

defines a second-order matrix pencil

$$\mathcal{P}(\lambda) = \mathbf{g}_{/\mathbf{y}} + \lambda\mathbf{g}_{/\dot{\mathbf{y}}} + \lambda^2\mathbf{g}_{/\ddot{\mathbf{y}}}. \tag{11}$$

According to the definition of DAE (see for example [20]), the pencil of Eq. (11) is non-singular for $\|\lambda\| < \infty$, except when λ is equal to the eigenvalues of the pencil, even when matrix $\mathbf{g}_{/\ddot{\mathbf{y}}}$ is singular. Thus $\mathbf{g}$, as in the case of constrained dynamics, is differential-algebraic.

When the problem is solved numerically using implicit integration schemes, a linear relationship exists between the variable increment and its derivatives, $\delta\dot{\mathbf{y}} = c_1\delta\ddot{\mathbf{y}}$, $\delta\mathbf{y} = c_2\delta\ddot{\mathbf{y}}$. For example, when Newmark's algorithm,

$$\dot{\mathbf{y}}_k = \dot{\mathbf{y}}_{k-1} + h\left(\gamma\ddot{\mathbf{y}}_k + (1-\gamma)\ddot{\mathbf{y}}_{k-1}\right) \tag{12a}$$

$$\mathbf{y}_k = \mathbf{y}_{k-1} + h\dot{\mathbf{y}}_{k-1} + \frac{h^2}{2}\left(2\beta\ddot{\mathbf{y}}_k + (1-2\beta)\ddot{\mathbf{y}}_{k-1}\right), \tag{12b}$$

is used, $c_1 = \gamma h$ and $c_2 = \beta h^2$ (when $\gamma = 1/2$ and $\beta = 1/4$ the method does not introduce algorithmic dissipation, and $c_2 = c_1^2$; in such case, however, the method cannot be used to integrate a DAE problem). In general, $c_1 \propto h$ and $c_2 \propto h^2$. In this work, an original method with tunable algorithmic dissipation is used [14], for which $c_1 = 2h/(4-(1-\rho_\infty)^2)$, where ρ_∞ is the asymptotic spectral radius of the method, and $c_2 = c_1^2$. The method is A-stable[2], and L-stable when $\rho_\infty = 0$; in such case, it corresponds to second-order Backward-Difference Formulas (BDF).

The correction phase of a predictor-corrector scheme for the approximation of the problem over a finite time step h requires one to solve a sequence of Newton-like iterations of the form

$$\left(c_2\mathbf{g}_{/\mathbf{y}} + c_1\mathbf{g}_{/\dot{\mathbf{y}}} + \mathbf{g}_{/\ddot{\mathbf{y}}}\right)\delta\ddot{\mathbf{y}} = -\mathbf{g}. \tag{13}$$

The matrix of Eq. (13), in analogy with the matrix pencil $\mathcal{P}(\lambda)$ of Eq. (11), is non-singular, with the possible exception of a finite set of values of c_1 and c_2.

For the sake of simplicity, consider a linear problem where $\mathbf{f} = -\mathbf{K}\mathbf{x} - \mathbf{D}\dot{\mathbf{x}}$ and $\mathbf{M}$, $\boldsymbol{\phi}_{/\mathbf{x}}$ and $\mathbf{B}$ do not depend on $\mathbf{x}$. The problem can be rearranged as

$$\left(c_2\begin{bmatrix}\mathbf{K}&\mathbf{0}&\mathbf{0}\\ \mathbf{0}&\mathbf{0}&\mathbf{0}\\ \mathbf{0}&\mathbf{0}&\mathbf{0}\end{bmatrix} + c_1\begin{bmatrix}\mathbf{D}&\mathbf{0}&\mathbf{0}\\ \mathbf{0}&\mathbf{0}&\mathbf{0}\\ \mathbf{0}&\mathbf{0}&\mathbf{0}\end{bmatrix} + \begin{bmatrix}\mathbf{M}&\boldsymbol{\phi}_{/\mathbf{x}}^T&-\mathbf{B}^T\\ \boldsymbol{\phi}_{/\mathbf{x}}&\mathbf{0}&\mathbf{0}\\ \boldsymbol{\psi}_{/\mathbf{x}}&\mathbf{0}&\mathbf{0}\end{bmatrix}\right)\begin{Bmatrix}\Delta\ddot{\mathbf{x}}\\ \Delta\boldsymbol{\lambda}\\ \Delta\mathbf{u}\end{Bmatrix} = \begin{Bmatrix}\mathbf{f} - \mathbf{M}\ddot{\mathbf{x}} - \boldsymbol{\phi}_{/\mathbf{x}}^T\boldsymbol{\lambda} + \mathbf{B}^T\mathbf{u}\\ -\boldsymbol{\phi}/c_2\\ (\boldsymbol{\alpha}-\boldsymbol{\psi})/c_2\end{Bmatrix} \tag{14}$$

As long as $c_1 \neq 0$ and $c_2 \neq 0$, even when the control realizability condition based on matrix $\mathbf{P}$ of Eq. (8a) being full rank is not met, a modified condition consisting in matrix

$$\mathbf{P}^* = \boldsymbol{\psi}_{/\mathbf{x}}\left(\mathbf{I} - \mathbf{H}\boldsymbol{\phi}_{/\mathbf{x}}^T\left(\boldsymbol{\phi}_{/\mathbf{x}}\mathbf{H}\boldsymbol{\phi}_{/\mathbf{x}}^T\right)^{-1}\boldsymbol{\phi}_{/\mathbf{x}}\right)\mathbf{H}\mathbf{B}^T \tag{15}$$

being full rank can be verified. Matrix $\mathbf{H} = (\mathbf{M} + c_1\mathbf{D} + c_2\mathbf{K})^{-1}$ is a sort of 'admittance' matrix, and matrix $\mathbf{P}^*$ results from the solution of Eq. (14) with respect to $\Delta\mathbf{u}$. This makes the realization of the control possible through the indirect effect of the control input on the constraint equation via the generalized compliance of the system discretized in time, including the contribution of all configuration-dependent forces, e.g. aerodynamic loads. In the general case, when a nonlinear problem is locally linearized to be solved iteratively, analogous considerations apply.

Considerations on Non-Minimum Phase Problems

The control constraint reduced admittance matrix $\hat{\mathbf{P}}^*(s) = s^2\boldsymbol{\psi}_{/\mathbf{q}}(s^2\hat{\mathbf{M}} + s\hat{\mathbf{D}} + \hat{\mathbf{K}})^{-1}\hat{\mathbf{B}}^T$, obtained in analogy with $\mathbf{P}^*$ considering the minimal coordinates $\mathbf{q}$, is said to have non-minimum phase when some of its zeros are in the

[2]See for example [21] for the definitions of A- and L-stability.

ASME J. Comput. Nonlinear Dyn. January 2011 6(1), doi:10.1115/1.4025629

right half of the complex plane. In this case, the control constraint is not feasible, despite $\hat{\mathbf{P}} = \lim_{s\to\infty} \hat{\mathbf{P}}^*(s)$ being non-singular, because the realization of the control constraint, which basically consists in an ideal zero-pole cancellation that completely cancels the dynamics of the problem, would not be causal.

However, the control input resulting from the evaluation of the discretized control constraint reduced admittance matrix with coefficients c_1 and c_2 resulting from a time step h that corresponds to a $s = j\omega = j2\pi/h$ below the smallest zero in the right half of the complex plane yields a control realization that overcomes the non-minimum phase initial behavior (i.e. the need of the system to initially respond in a direction opposite to the imposed trajectory). Intuitively, as long as a large enough time step is used, the initial non-causal response can be skipped. This poses a severe limitation on the applicability of the proposed approach to systems whose control constraint realization would otherwise be non-causal because the time step required to overcome the initial non-minimum phase response could be too long to yield acceptable results. However, with these caveats in mind, an example application of the control of a problem of this type is presented in a later section.

Applications

The proposed approach to control constraint realization has been implemented in the free general-purpose multibody software MBDyn (`http://www.mbdyn.org/`) since release 1.3 by introducing two specific elements: one, called 'total equation', enforces a set of up to 6 arbitrary relationships between the relative position, orientation, velocity and angular velocity of two structural nodes; the other, called 'total reaction', applies a corresponding set of Lagrange multipliers to the equations of motion of two other structural nodes. An arbitrary combination of multiple occurrences of each element can be used simultaneously in a model. The details of the implementation go beyond the scope of this paper; nonetheless, it is worth stressing that the whole functionality has been implemented by means of minimally intrusive modifications to the existing solver, namely by adding the two companion elements to the existing joint element library.

Planar Parallel Manipulator

This application, sketched in Fig. 1 top left, represents a free floating planar parallel manipulator loosely derived from the one presented by Betsch and co-workers [22, 23]. The original problem consisted of three sets of Revolute-Prismatic-Revolute (RPR) joints connecting two bodies, and was treated as planar. Since MBDyn only models three-dimensional systems, the analyzed model is three-dimensional, although only planar motion actually takes place. One platform, the inner triangle, is connected to three rigid bars by Cardano joints. Each of these bars can slide radially with respect to a point that is connected to the other platform, the outer triangle, by a spherical joint. Actuators #1, #2 and #3 in Fig. 1 are represented by the bullets at the top, on the right and on the left of the outer triangle, respectively. The in-plane motion of the inner triangle is controlled by applying a torque to each outer joint about an axis normal to the plane of the figure, reacted by the inertia of the outer triangle.

Table 1. Planar parallel manipulator data

Distance of inner revol. from center	d_i	0.5	m
Mass of inner triangle	m_i	3.0	kg
Inertia of inner triangle	J_i	2.0	kg·m^2
Distance of outer revol. from center	d_o	1.0	m
Mass of outer triangle	m_o	8.0	kg
Inertia of outer triangle	J_o	0.1	kg·m^2
Length of actuators	l_a	1.0	m
Mass of actuator	m_a	7.0	kg
Inertia of actuator	J_a	0.002	kg·m^2

The redundant coordinate model consists of 6 structural nodes (36 degrees of freedom, 66 states since the ground node has no inertia), 24 constraint equations and 3 control constraints. A minimal set approach would need 12 degrees of freedom (rigid body motion of the two triangles in space) and 3 control constraints. The control constraint realization is non-ideal orthogonal.

The prescribed motion constrains the trajectory of the center of mass of the inner triangle, with no rotation. Since no external forces are applied, the linear and angular momentum of the overall system must not change. The properties of the problem are illustrated in Table 1. In the initial configuration the Center of Mass (CM) of each bar is in the corresponding outer revolute joint, which is actually modeled as a spherical joint to avoid overconstraining the model.

The trajectory of the center of the inner platform, a lemniscate-like 'eight'-shaped path, is enforced according to the law

$$x_{\mathrm{CM}} = \frac{1}{6}\sin(\theta(t)), \quad y_{\mathrm{CM}} = \frac{1}{8}\sin(2\theta(t)), \quad \psi = 0 \tag{16}$$

with

$$n(\xi) = 21\xi^6 - 60\xi^7 + 67.5\xi^8 - 35\xi^9 + 7\xi^{10}$$

$$\theta(t) = (T_1 - T_0)\, n\left(\frac{t - T_0}{T_1 - T_0}\right)\omega_0,\ T_0 \le t \le T_1 \tag{17a}$$

$$\theta(t) = \theta(T_1) + (t - T_1)\,\omega_0,\ T_1 \le t \le T_2 \tag{17b}$$

$$\theta(t) = \theta(T_2) + (T_3 - T_2)\, n\left(\frac{t - T_2}{T_3 - T_2}\right)\omega_0,\ T_2 \le t \le T_3, \tag{17c}$$

$T_0 = 0$ s, $T_1 = 1$ s, $T_2 = 2$ s, $T_3 = 3$ s, and $\omega_0 = \pi$ radian/s. Figure 1 also presents three snapshots of the configuration of the manipulator during the simulation.

Figure 2 shows the trajectory of the CM of the two platforms. Figure 3 shows the time history of the trajectory of the CM and of the rotation of the two platforms. Note how they start and end at zero, with horizontal slope. Figures 4 and 5 show the time histories of the torque and the rotation of the actuators.

ASME J. Comput. Nonlinear Dyn. January 2011 6(1), doi:10.1115/1.4025629

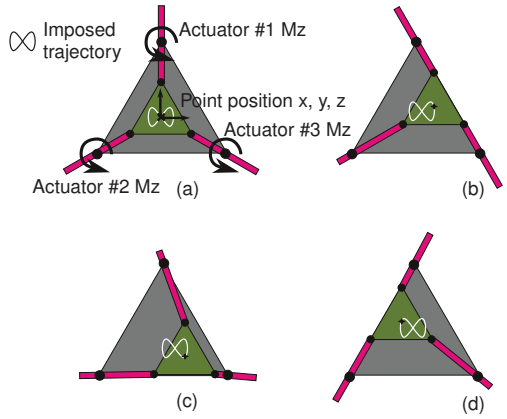

Fig. 1. Snapshots of planar parallel manipulator at t = 0.0 s (a), 0.9 s (b), 1.2 s (c) and 1.8 s (d).

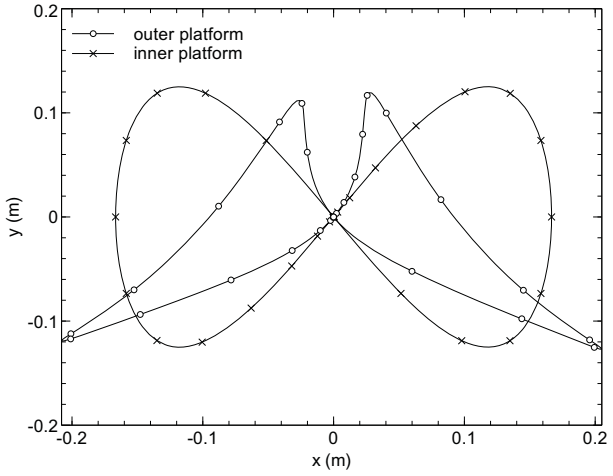

Fig. 2. CM trajectory of both platforms.

Trajectory Control of Canard Aircraft

This problem consists in controlling the trajectory in the vertical plane of a simplified model of an aircraft (Fig. 6) by controlling the pitch of a canard lifting surface, whose positive actuation directly induces an increase in total lift of the aircraft. The control input is the torque applied to the canard surface about the pitch axis; by pitching it, the lift of the canard changes accordingly, producing a pitching moment that causes the pitching of the aircraft. In turn, the pitching of the aircraft changes the pitch of the main wing as well. The combined effect is a change in total lift that accelerates the aircraft in the direction required to comply with the control constraint.

The structural and aerodynamic properties of the aircraft are listed in Table 2. Two rigid bodies are used for the aircraft and the canard surface. The two bodies are constrained by a revolute joint that only allows the relative pitch rotation. The pitch and heave motion of the aircraft are unconstrained. The maneuver consists in changing the altitude of the aircraft by 100 m in 10 seconds. The vertical trajec-

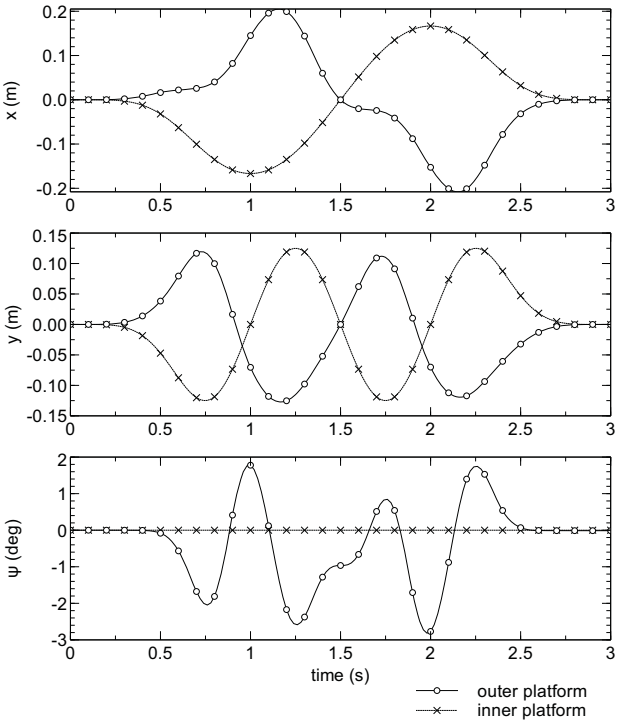

Fig. 3. CM motion and rotation of both platforms.

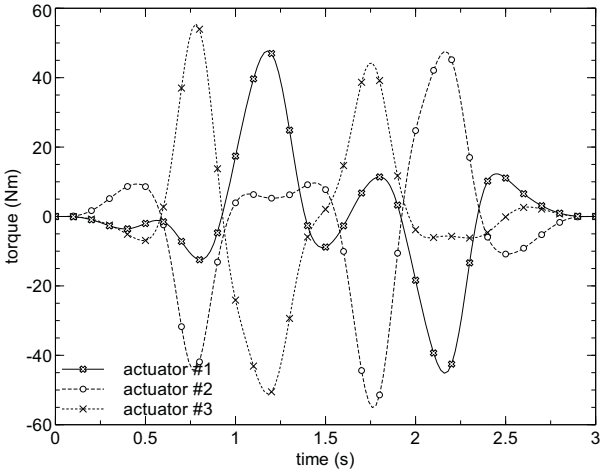

Fig. 4. Torque in actuators.

Table 2. Canard data

Aircraft mass	M_a	50.0	kg
Aircraft inertia about CM	J_a	10.0	kg·m^2
Canard mass	M_c	1.0	kg
Wing surface	S_w	0.2	m^2
Canard surface	S_c	0.02	m^2
Wing center from CM	d_w	0.1	m
Canard center from CM	d_c	-0.8	m
Airfoil		NACA 0012	
Airstream velocity	V_∞	170.0	kts
Air density	ρ	1.225	kg·m^{-3}
Gravity	g	9.81	m·s^{-2}

ASME J. Comput. Nonlinear Dyn. January 2011 6(1), doi:10.1115/1.4025629

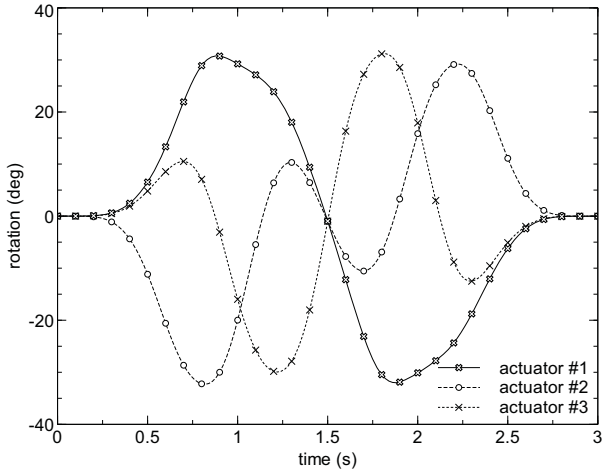

Fig. 5. Rotation of actuators.

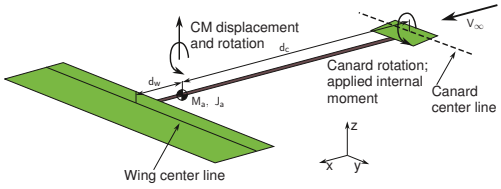

Fig. 6. Canard: sketch.

tory of the aircraft is prescribed by a constraint. The corresponding multiplier applies an internal reaction torque to the canard pitch equilibrium equation.

The redundant coordinate model consists of 3 structural nodes (18 degrees of freedom, 30 states), 15 constraint equations and one control constraint. A minimal set approach would need 3 degrees of freedom (aircraft pitch and heave, and canard rotation) and one control constraint. The control realization is tangent; only the dependence of the aerodynamic forces on the pitch rotation of the control surface can directly affect the acceleration of the aircraft in the direction of the prescribed motion.

The pitch rotation of the canard thus indirectly controls the vertical component of the position of the aircraft according to

$$f(t) = f_0 + \left(126\left(\frac{t}{T}\right)^5 - 420\left(\frac{t}{T}\right)^6 + 540\left(\frac{t}{T}\right)^7 - 315\left(\frac{t}{T}\right)^8 + 70\left(\frac{t}{T}\right)^9\right)(f_1 - f_0), \qquad (18)$$

continuous up to the fourth order derivative, with $f_0 = 0$ m, $f_1 = 100$ m, $T = 10$ s. The horizontal component of the velocity is directly constrained.

The quality of the result has been verified by imposing the relative pitch rotation of the canard surface resulting from the control constraint analysis to a direct simulation with the same model, in nominal and perturbed conditions, without and with feedforward and feedback control. Feedback control imposes to the canard surface an additional rotation proportional to the elevation and climb rate errors,

$$\theta_c = \theta_{\text{ff}} - K_p \Delta z - K_d \Delta \dot{z} \qquad (19)$$

with $K_p = 0.002$ radian·m^{-1} and $K_d = 0.002$ radian·s·m^{-1}; Δz is the difference between the actual and prescribed vertical position.

Figure 7 (top) shows the imposed vertical component of the position of the aircraft (the curve marked 'control constraint'), the one resulting from the application of feedback control only ($\theta_{\text{ff}} = 0$, curve marked 'no f.f., PD'), the one obtained with feedforward control applied to the baseline model ('f.f., baseline', coincident with the first one), and those resulting from the application of feedforward control to a model with a $\pm 5\%$ perturbation of the mass of the aircraft, including a corresponding shift of the center of mass (respectively 'f.f., $\pm 5\%$ mass'). Figure 7 (bottom) shows the difference between various mass configurations of the aircraft with combined feedforward and feedback control (in the combined feedforward/feedback cases only the difference is shown, otherwise it would be indistinguishable from the nominal case). Figures 8 and 9 show the corresponding attitude of the aircraft and canard surface pitch for the above illustrated configurations.

The results show that the feedforward control designed by the proposed procedure is very effective and robust when combined with a simple feedback correction. The same feedback alone would result in a fairly poor capability to accomplish the prescribed task. Note that in the presence of a significant perturbation of the model (5% of the mass), the prescribed trajectory is performed within 0.5% using feedforward and feedback control, at the cost of a 25% larger control motion. Note also that a significant fraction of the difference between the feedforward and the actual control motion (± 0.2 deg before and after the maneuver) is related to compensating for the different trim condition associated with the mass perturbation.

Trajectory Control of Conventional Aircraft

When a conventional aircraft is considered (Fig. 10), the corresponding linearized problem is non-minimum phase, since a deflection of the control surface on the tail that directly increases the lift eventually induces a pitching of the aircraft that reduces the overall lift. However, by choosing an adequately long time step, the initial non-causal behavior required to control the aircraft can be avoided. The model structure is the same of the previous case, as well as the data, with the only exception of the tail surface, whose aerodynamic center is located at a distance $d_t = 0.8$ m from the CM of the aircraft. When a time step $h = 0.5$ s is used, the control constraint for a desired trajectory analogous to that of the previous case ($\Delta z = 100$ m in 12 s) can be successfully realized, resulting in a very coarse determination of the required feedforward command. The subsequent verification, with a finer time step $h = 0.01$ s and a linear interpolation of the feedforward command, drifts significantly unless compensated by proportional-derivative feedback, as shown in

ASME J. Comput. Nonlinear Dyn. January 2011 6(1), doi:10.1115/1.4025629

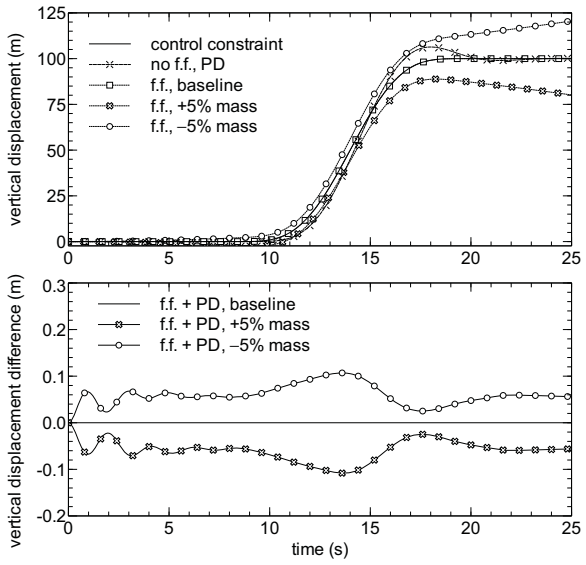

Fig. 7. Canard: vertical motion (top); difference (bottom).

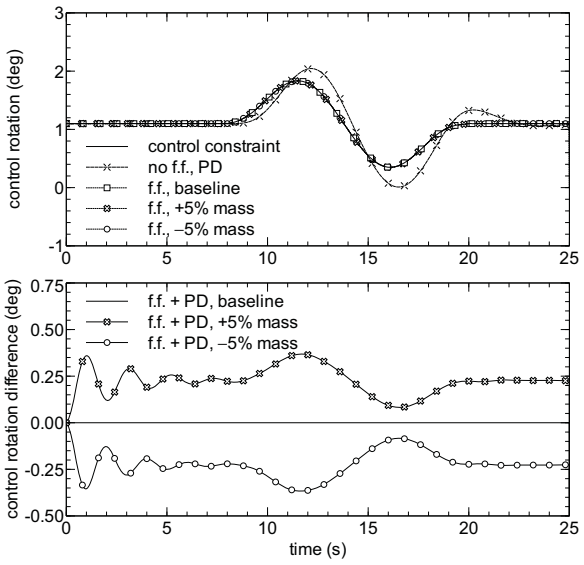

Fig. 9. Canard: control rotation (top); difference (bottom).

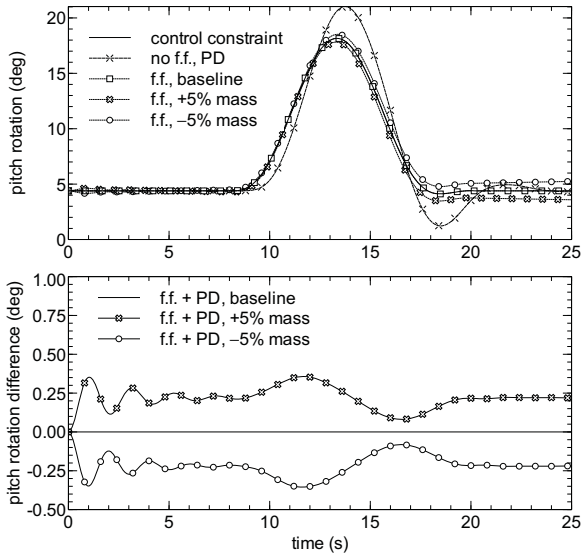

Fig. 8. Canard: pitch rotation (top); difference (bottom).

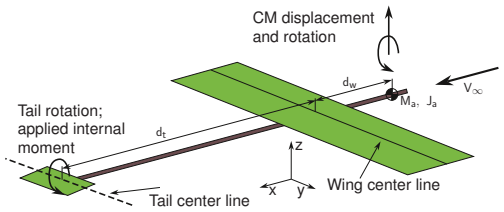

Fig. 10. Conventional aircraft: sketch.

Table 3. Horizontal axis wind turbine data

Hub height	h	35.0	m
Number of blades	N_b	3	
Blade mass	M_b	100.0	kg
Blade radius	R	20.0	m
Blade root cutout	R_{cutout}	2.0	m
Blade root chord	c_{root}	2.0	m
Blade tip chord	c_{tip}	0.5	m
Airfoil		NACA 0012	
Reference wind velocity	V_∞	10.0	$\text{m}\cdot\text{s}^{-1}$
Air density	ρ	1.225	$\text{kg}\cdot\text{m}^{-3}$
Gravity	g	9.81	$\text{m}\cdot\text{s}^{-2}$

Figure 11; Figure 12 shows the corresponding control rotation. This result, unpublished so far to the authors' knowledge, is quite interesting and promising.

Control of Wind Turbine Angular Velocity

The angular velocity Ω of a simplified yet complete model of a Horizontal Axis Wind Turbine (HAWT), shown in Fig. 13, is controlled by acting on the collective pitch of the blades. The structural and aerodynamic properties are listed in Table 3. The redundant coordinate model consists of 6 structural nodes (36 degrees of freedom, 66 states), 34 constraint equations and one control constraint. A minimal set approach would need 2 degrees of freedom (wind turbine rotation, pitch control displacement) and one control constraint. The control realization is tangent; only the dependence of the aerodynamic forces on the pitch of the blades can directly affect the angular acceleration of the turbine in the direction of the prescribed motion.

The feedforward control is designed to change the angular velocity in steady wind from an initial value $\Omega_0 = 60$

ASME J. Comput. Nonlinear Dyn. January 2011 6(1), doi:10.1115/1.4025629

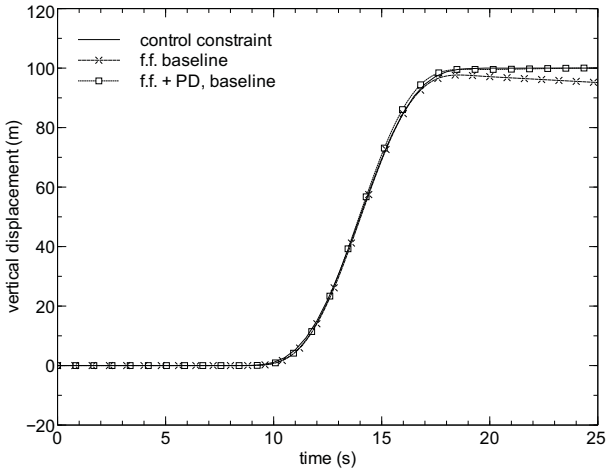

Fig. 11. Conventional aircraft: vertical motion.

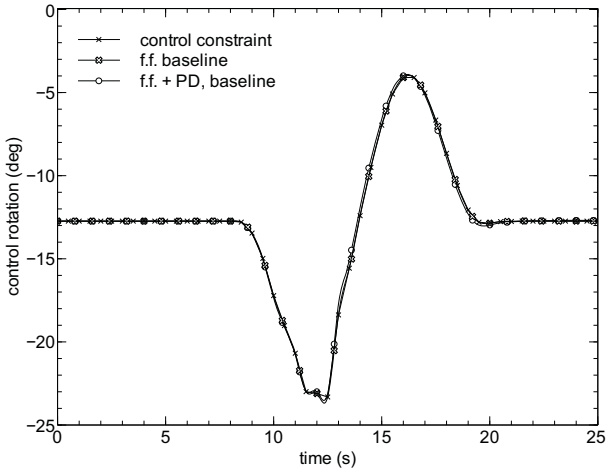

Fig. 12. Conventional aircraft: control rotation.

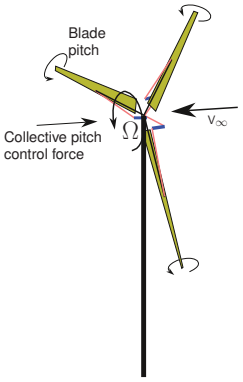

Fig. 13. HAWT: sketch.

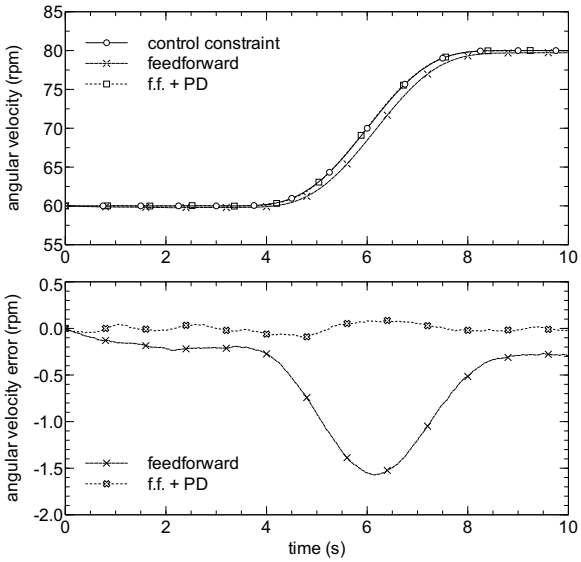

Fig. 14. HAWT: angular velocity.

rpm to a final value $\Omega_f = 80$ rpm in 6 seconds, according to Eq. (18). Different types of disturbances and model imperfections have been considered.

Actuator dynamics: The motion imposed to the pitch control actuators is filtered by the function

$$x_{\text{out}} = \frac{\omega_0^2}{s^2 + 2\xi\omega_0 s + \omega_0^2} x_{\text{in}} \tag{20}$$

with $\omega_0 = 4\pi$ and $\xi = 1$, i.e. a low-pass filter with cut frequency at 2Hz.

Wind profile: the unrealistic uniform flow used when designing the feedforward law is replaced in the verification by a more realistic 'power law' wind profile [24], with additional random disturbances, simulating the natural turbulence of the flow. The wind profile is $v = v_{\text{ref}}(z/z_{\text{ref}})^p$, with $v_{\text{ref}} = V_\infty$, $z_{\text{ref}} = h$ and $p = 0.17$, a typical value for wind over flat soil.

Figure 14 shows the time history of the angular velocity of the turbine, while Fig. 15 shows the related collective pitch control. The line marked 'feedforward' refers to the analysis of a model with feedforward control that includes the dynamics of the actuator and power law wind profile with random gust. The actuator dynamics causes an appreciable delay in the response of the system. The proportional/derivative feedback that corrects the blade pitch based on the error between the actual and the prescribed angular velocity and its derivative makes it possible to obtain the desired behavior with minimal error, as shown by the lines marked 'f.f. + PD'.

Conclusions

This paper discusses the application of control constraint to non-trivial under-actuated systems modeled using the multibody formalism. Conditions for the realization of the control are formulated; specifically, an alternative condition for the orthogonal realization of the control constraint based on the control constraint Jacobian matrix and on the

ASME J. Comput. Nonlinear Dyn. January 2011 6(1), doi:10.1115/1.4025629

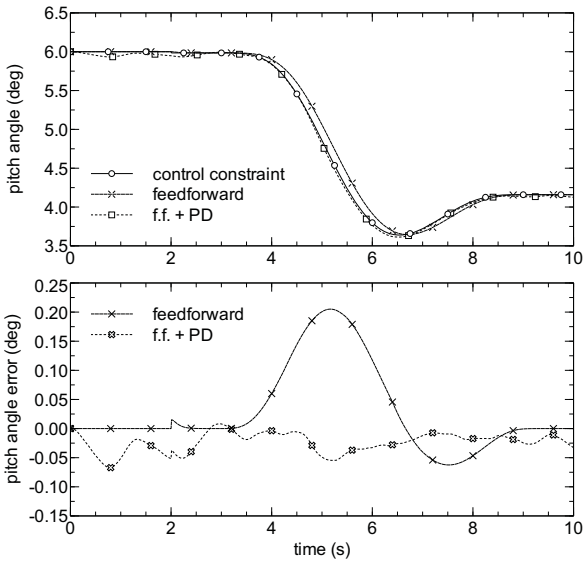

Fig. 15. HAWT: blade collective pitch.

control input matrix has been formulated. The equivalence of realization conditions for minimal and redundant coordinate set formulations is shown. Simple yet complete problems are solved using a general-purpose multibody formulation without resorting to any explicit index reduction. The soundness of the approach is illustrated by numerical examples of non trivial complexity, where the control input is determined first. The validity of the computed control is subsequently verified by both feedforwarding it in the system directly and with feedback to compensate for disturbances and model errors. The application of the proposed approach to non-minimum phase problems has been briefly discussed and verified considering the trajectory control of a conventional aircraft configuration along the vertical axis.

Acknowledgments

With the contribution of *Ministero degli Affari Esteri*, *Direzione Generale per la Promozione del Sistema Paese*.

References

[1] Laulusa, A. and Bauchau, O. A., 2008, "Review of classical approaches for constraint enforcement in multibody systems," J. of Computational and Nonlinear Dynamics, **3**(1), doi:10.1115/1.2803257.

[2] Bauchau, O. A. and Laulusa, A., 2008, "Review of contemporary approaches for constraint enforcement in multibody systems," J. of Computational and Nonlinear Dynamics, **3**(1), doi:10.1115/1.2803258.

[3] Chen, Y.-H., 2005, "Mechanical systems under servo constraints: the Lagrange's approach," Mechatronics, **15**(3), pp. 317–337, doi:10.1016/j.mechatronics.2004.09.003.

[4] Chen, Y.-H., 2008, "Equations of motion of mechanical systems under servo constraints: the Maggi approach," Mechatronics, **18**(4), pp. 208–217, doi:10.1016/j.mechatronics.2007.12.004.

[5] Blajer, W. and Kołodziejczyk, K., 2007, "Control of underactuated mechanical systems with servo-constraints," Nonlinear Dynamics, **50**(4), pp. 781–791, doi:10.1007/s11071-007-9231-4.

[6] Blajer, W. and Kołodziejczyk, K., 2004, "A geometric approach to solving problem of control constraints: Theory and a DAE framework," Multibody System Dynamics, **11**(4), pp. 343–364, doi:10.1023/B:MUBO.0000040800.40045.51.

[7] Wang, J. T., 1990, "Inverse dynamics of constrained multibody systems," Journal of Applied Mechanics, **57**(3), pp. 750–757, doi:10.1115/1.2897087.

[8] Blajer, W., 1997, "Dynamics and control of mechanical systems in partly specified motion," J. Franklin Institute, **334**(3), pp. 407–426, doi:10.1016/S0016-0032(96)00091-9.

[9] Lam, S., 1998, "On Lagrangian dynamics and its control formulations," Applied Mathematics and Computation, **91**(2–3), pp. 259–284, doi:10.1016/S0096-3003(97)10004-2.

[10] Rosen, A., 1999, "Applying the Lagrange method to solve problems of control constraints," Journal of Applied Mechanics, **66**(4), pp. 1013–1015, doi:10.1115/1.2791770.

[11] Gobulev, Y., 2001, "Mechanical systems with servoconstraints," J. Appl. Maths. Mechs., **65**(2), pp. 205–217, doi:10.1016/S0021-8928(01)00024-7.

[12] Blajer, W. and Kołodziejczyk, K., 2008, "Modeling of underactuated mechanical systems in partly specified motion," Journal of Theoretical and Applied Mechanics, **46**(2), pp. 383–394.

[13] Blajer, W. and Kołodziejczyk, K., 2011, "Improved DAE formulation for inverse dynamics simulation of cranes," Multibody System Dynamics, **25**(2), pp. 131–143, doi:10.1007/s11044-010-9227-6.

[14] Fumagalli, A., Masarati, P., Morandini, M., and Mantegazza, P., 2011, "Control constraint realization for multibody systems," J. of Computational and Nonlinear Dynamics, **6**(1), p. 011002 (8 pages), doi:10.1115/1.4002087.

[15] Singh, R. P. and Likins, P. W., 1985, "Singular value decomposition for constrained dynamical systems," J. Appl. Mech., **52**(4), pp. 943–948, doi:10.1115/1.3169173.

[16] Mani, N. K., Haug, E. J., and Atkinson, K. E., 1985, "Application of singular value decomposition for analysis of mechanical system dynamics," J. Mech. Trans. Auto. Des., **107**(1), pp. 82–87, doi:10.1115/1.3258699.

[17] Kim, S. S. and Vanderploeg, M. J., 1986, "QR decomposition for state space representation of constrained mechanical dynamic systems," J. of Mech. Trans., **108**(2), pp. 183–188, doi:10.1115/1.3260800.

[18] Blajer, W., 2001, "A geometrical interpretation and uniform matrix formulation of multibody system dynamics," ZAMM — Journal of Applied Mathematics and Mechanics, **81**(4), pp. 247–259, doi:10.1002/1521-4001(200104)81:4<247::AID-ZAMM247>3.0.CO;2-D.

[19] Pennestrì, E. and Vita, L., 2004, "Strategies for the numerical integration of DAE systems in multibody dynamics," Computer Applications in Engineering Education, **12**(2), pp. 106–116, doi:10.1002/cae.20005.

[20] Brenan, K. E., Campbell, S. L. V., and Petzold, L. R., 1989, *Numerical Solution of Initial-Value Problems in Differential-Algebraic Equations*, North-Holland, New York.

[21] Lambert, J. D., 1991, *Numerical Methods for Ordinary Differential Systems*, John Wiley & Sons Ltd., Chichester, Eng-

land.
[22] Uhlar, S. and Betsch, P., 2008, "Conserving integrators for parallel manipulators," *Parallel Manipulators*, J.-H. Ryu, ed., chap. 5, I-Tech Education and Publishing, www.books.i-techonline.com, Vienna, Austria, pp. 75–108.
[23] Betsch, P., Uhlar, S., Saeger, N., Siebert, R., and Franke, M., 2010, "Benefits of a rotationless rigid body formulation to computational flexible multibody dynamics," *1st ESA Workshop on Multibody Dynamics for Space Applications*, ESTEC, Noordwijk, NL.
[24] Panofsky, H. A. and Dutton, J. A., 1984, *Atmospheric turbulence: models and methods for engineering aplications*, John Wiley & Sons, New York.

Appendix: Equivalence of Control Realizability Conditions

The equivalence of the control realizability conditions given by matrices $\hat{\mathbf{P}}$ of Eq. (5) and $\mathbf{P}$ of Eq. (8a) is verified. Consider the Generalized Moore-Penrose Inverse (GMPI) of matrices $\boldsymbol{\vartheta}_{/\mathbf{q}}$ and $\boldsymbol{\phi}_{/\mathbf{x}}$,

$$\boldsymbol{\vartheta}^{+}_{/\mathbf{q}} = \left(\boldsymbol{\vartheta}^{T}_{/\mathbf{q}}\boldsymbol{\vartheta}_{/\mathbf{q}}\right)^{-1}\boldsymbol{\vartheta}^{T}_{/\mathbf{q}} \tag{21a}$$

$$\boldsymbol{\phi}^{+}_{/\mathbf{x}} = \boldsymbol{\phi}^{T}_{/\mathbf{x}}\left(\boldsymbol{\phi}_{/\mathbf{x}}\boldsymbol{\phi}^{T}_{/\mathbf{x}}\right)^{-1}. \tag{21b}$$

If the constraint Jacobian matrix $\boldsymbol{\phi}_{/\mathbf{x}}$ is full row rank, i.e. constraints are not redundant, both pseudo-inverses are full column rank as well.

Consider the invertible transformation matrix

$$\mathbf{T} = \left[\boldsymbol{\vartheta}_{/\mathbf{q}}\ \boldsymbol{\phi}^{+}_{/\mathbf{x}}\right]; \tag{22}$$

its inverse is

$$\mathbf{T}^{-1} = \begin{bmatrix}\boldsymbol{\vartheta}^{+}_{/\mathbf{q}}\\ \boldsymbol{\phi}_{/\mathbf{x}}\end{bmatrix}. \tag{23}$$

In fact, one can easily verify that, since by definition $\boldsymbol{\phi}_{/\mathbf{x}}\boldsymbol{\vartheta}_{/\mathbf{q}} = \mathbf{0}$, then

$$\mathbf{T}^{-1}\mathbf{T} = \begin{bmatrix}\boldsymbol{\vartheta}^{+}_{/\mathbf{q}}\boldsymbol{\vartheta}_{/\mathbf{q}} & \boldsymbol{\vartheta}^{+}_{/\mathbf{q}}\boldsymbol{\phi}^{+}_{/\mathbf{x}}\\ \boldsymbol{\phi}_{/\mathbf{x}}\boldsymbol{\vartheta}_{/\mathbf{q}} & \boldsymbol{\phi}_{/\mathbf{x}}\boldsymbol{\phi}^{+}_{/\mathbf{x}}\end{bmatrix} = \begin{bmatrix}\mathbf{I} & \mathbf{0}\\ \mathbf{0} & \mathbf{I}\end{bmatrix} = \mathbf{I}. \tag{24}$$

As a consequence, since Eq. (24) implies that $\mathbf{T}\mathbf{T}^{-1} = \mathbf{I}$, then

$$\boldsymbol{\vartheta}_{/\mathbf{q}}\boldsymbol{\vartheta}^{+}_{/\mathbf{q}} + \boldsymbol{\phi}^{+}_{/\mathbf{x}}\boldsymbol{\phi}_{/\mathbf{x}} = \mathbf{T}\mathbf{T}^{-1} = \mathbf{I}. \tag{25}$$

Transform the (symmetric, positive definite) mass matrix $\mathbf{M}$ using $\mathbf{T}$, namely $\overline{\mathbf{M}} = \mathbf{T}^{T}\mathbf{M}\mathbf{T}$. The inverse of $\overline{\mathbf{M}}$ is

$$\begin{aligned}\overline{\mathbf{M}}^{-1} = \mathbf{T}^{-1}\mathbf{M}^{-1}\mathbf{T}^{-T} &= \begin{bmatrix}\boldsymbol{\vartheta}^{+}_{/\mathbf{q}}\mathbf{M}^{-1}\left(\boldsymbol{\vartheta}^{+}_{/\mathbf{q}}\right)^{T} & \boldsymbol{\vartheta}^{+}_{/\mathbf{q}}\mathbf{M}^{-1}\boldsymbol{\phi}^{T}_{/\mathbf{x}}\\ \boldsymbol{\phi}_{/\mathbf{x}}\mathbf{M}^{-1}\left(\boldsymbol{\vartheta}^{+}_{/\mathbf{q}}\right)^{T} & \boldsymbol{\phi}_{/\mathbf{x}}\mathbf{M}^{-1}\boldsymbol{\phi}^{T}_{/\mathbf{x}}\end{bmatrix}\\ &= \begin{bmatrix}\hat{\mathbf{N}} & \mathbf{N}^{T}_{\mathbf{xq}}\\ \mathbf{N}_{\mathbf{xq}} & \mathbf{N}_{\mathbf{xx}}\end{bmatrix}.\end{aligned} \tag{26}$$

According to the matrix inversion lemma, $\hat{\mathbf{M}}^{-1} = \left(\boldsymbol{\vartheta}^{T}_{/\mathbf{q}}\mathbf{M}\boldsymbol{\vartheta}_{/\mathbf{q}}\right)^{-1}$ can be written in terms of $\overline{\mathbf{M}}^{-1}$ as

$$\begin{aligned}\hat{\mathbf{M}}^{-1} &= \hat{\mathbf{N}} - \mathbf{N}^{T}_{\mathbf{xq}}\mathbf{N}^{-1}_{\mathbf{xx}}\mathbf{N}_{\mathbf{xq}}\\ &= \boldsymbol{\vartheta}^{+}_{/\mathbf{q}}\mathbf{M}^{-1}\left(\boldsymbol{\vartheta}^{+}_{/\mathbf{q}}\right)^{T}\\ &\quad - \boldsymbol{\vartheta}^{+}_{/\mathbf{q}}\mathbf{M}^{-1}\boldsymbol{\phi}^{T}_{/\mathbf{x}}\left(\boldsymbol{\phi}_{/\mathbf{x}}\mathbf{M}^{-1}\boldsymbol{\phi}^{T}_{/\mathbf{x}}\right)^{-1}\boldsymbol{\phi}_{/\mathbf{x}}\mathbf{M}^{-1}\left(\boldsymbol{\vartheta}^{+}_{/\mathbf{q}}\right)^{T}\\ &= \boldsymbol{\vartheta}^{+}_{/\mathbf{q}}\left(\mathbf{M}^{-1} - \mathbf{M}^{-1}\boldsymbol{\phi}^{T}_{/\mathbf{x}}\left(\boldsymbol{\phi}_{/\mathbf{x}}\mathbf{M}^{-1}\boldsymbol{\phi}^{T}_{/\mathbf{x}}\right)^{-1}\boldsymbol{\phi}_{/\mathbf{x}}\mathbf{M}^{-1}\right)\left(\boldsymbol{\vartheta}^{+}_{/\mathbf{q}}\right)^{T}.\end{aligned} \tag{27}$$

Matrix $\boldsymbol{\psi}_{/\mathbf{q}}\hat{\mathbf{M}}^{-1}\hat{\mathbf{B}}^{T}$ can be written as

$$\boldsymbol{\psi}_{/\mathbf{q}}\hat{\mathbf{M}}^{-1}\hat{\mathbf{B}}^{T} = \boldsymbol{\psi}_{/\mathbf{x}}\boldsymbol{\vartheta}_{/\mathbf{q}}\hat{\mathbf{M}}^{-1}\boldsymbol{\vartheta}^{T}_{/\mathbf{q}}\mathbf{B}^{T}; \tag{28}$$

thus

$$\begin{aligned}&\boldsymbol{\vartheta}_{/\mathbf{q}}\hat{\mathbf{M}}^{-1}\boldsymbol{\vartheta}^{T}_{/\mathbf{q}} =\\ &\boldsymbol{\vartheta}_{/\mathbf{q}}\boldsymbol{\vartheta}^{+}_{/\mathbf{q}}\left(\mathbf{M}^{-1} - \mathbf{M}^{-1}\boldsymbol{\phi}^{T}_{/\mathbf{x}}\left(\boldsymbol{\phi}_{/\mathbf{x}}\mathbf{M}^{-1}\boldsymbol{\phi}^{T}_{/\mathbf{x}}\right)^{-1}\boldsymbol{\phi}_{/\mathbf{x}}\mathbf{M}^{-1}\right)\left(\boldsymbol{\vartheta}_{/\mathbf{q}}\boldsymbol{\vartheta}^{+}_{/\mathbf{q}}\right)^{T}.\end{aligned} \tag{29}$$

By exploiting the property of Eq. (25), $\boldsymbol{\vartheta}_{/\mathbf{q}}\boldsymbol{\vartheta}^{+}_{/\mathbf{q}} = \mathbf{I} - \boldsymbol{\phi}^{+}_{/\mathbf{x}}\boldsymbol{\phi}_{/\mathbf{x}}$, i.e. $\boldsymbol{\vartheta}_{/\mathbf{q}}\boldsymbol{\vartheta}^{+}_{/\mathbf{q}}$ is an orthogonal projector. This proves that

$$\boldsymbol{\vartheta}_{/\mathbf{q}}\hat{\mathbf{M}}^{-1}\boldsymbol{\vartheta}^{T}_{/\mathbf{q}} = \mathbf{M}^{-1} - \mathbf{M}^{-1}\boldsymbol{\phi}^{T}_{/\mathbf{x}}\left(\boldsymbol{\phi}_{/\mathbf{x}}\mathbf{M}^{-1}\boldsymbol{\phi}^{T}_{/\mathbf{x}}\right)^{-1}\boldsymbol{\phi}_{/\mathbf{x}}\mathbf{M}^{-1}, \tag{30}$$

and thus the equivalence between the control realization condition of the minimal and redundant coordinate set formulations.